Proceedings of the 11th Brazilian Congress of Thermal Sciences and Engineering -- ENCIT 2006
Braz. Soc. of Mechanical Sciences and Engineering -- ABCM, Curitiba, Brazil, Dec. 5-8, 2006

Paper CIT06-0359

INVERSE BOUNDARY DESIGN IN HEAT TRANSFER COMBINING TURBULENT CONVECTION AND THERMAL RADIATION

Anderson C. Mossi
Federal University of Rio Grande do Sul, UFRGS
mossi@mecanica.ufrgs.br

Horácio A. Vielmo
Federal University of Rio Grande do Sul, UFRGS
vielmoh@mecanica.ufrgs.br

Francis H. R. França
Federal University of Rio Grande do Sul, UFRGS
frfranca@mecanica.ufrgs.br

Abstract. *This work investigates the solutions of an inverse boundary design problem which has multimode (radiation and convection) heat transfer mechanisms. The problem consists of finding the heat flux distribution required on heaters located on the top and side walls of a two-dimensional enclosure that satisfies both the temperature and heat flux distributions prescribed on the design surface of the enclosure. A turbulent air flow is generated by a fan located inside the chamber. The walls are gray, diffuse emitters and absorbers. The combined heat transfer problem is described by a system of non-linear equations, which is expected to be ill-conditioned as an inverse analysis is involved. The system of equations is solved by an iterative procedure: the basic set of equations relates the radiation transferred between the heater and the design surface, while all the other terms involved in the energy exchange are found from the conditions of the previous iteration. This way, the ill-posed part of the problem (which arises from the design surfaces containing two conditions, and the heater elements being unconstrained) is isolated for a more effective treatment. The solution is obtained by regularizing the ill-conditioned system of equations by means of the truncated singular value decomposition (TSVD) method.*

Keywords*. Inverse Design, Combined Heat Transfer, Turbulent Convection, Thermal Radiation, TSVD Regularization.*

1. Introduction

Many industrial processes, such as in the metallurgy field and the rapid thermal processing of silicon wafers, require controlled heating of materials. For instance, in thermal processing of materials, uniformity of temperature is often required to avoid thermal stresses and allow a better control of several manufacturing processes. This can be achieved only by means of a carefully controlled heat flux on the surface of the processed material, as governed by the energy balance, so that both the temperature and heat flux are imposed. The thermal designer aims at finding the thermal conditions of the system such that these two conditions are simultaneously satisfied.

In the inverse design approach, the conditions in the unconstrained elements are found directly from the two specifications on the design surface, avoiding the trial-and-error procedure of the forward design. The mathematical model allows the prescription of two conditions in some boundaries while other regions are left unconstrained. For problems that involve thermal radiation heat transfer, this type of formulation is described by a Fredholm integral equation of the first kind, known to result in ill-posed problems that can be solved only by means of regularization methods (Hansen, 1990). A comprehensive review of steady state inverse design can be found in França et al. (2002), and recent contributions on transient inverse design can be found in Daun et al. (2006) and França and Howell (2006).

This paper considers an inverse boundary design of a two-dimensional rectangular enclosure where the heat transfer is governed by thermal radiation and turbulent convection. The objective is to find the heat input on the heater located on the top and side surfaces of the enclosure so that the temperature and the heat flux imposed on the design surface are both attained. All physical properties are assumed constant and all the surfaces that form the enclosure are gray emitters and absorbers. The energy transport is governed by radiation and turbulent forced convection. The fluid flow and the diffusive-advective terms of the energy equation are treated numerically by the control volume method, with the turbulent transport being described by the $k-\varepsilon$ model. The radiative terms are treated by the discretization of the surfaces into uniform-sized elements. Due to the different characteristics of the radiation and convection mechanisms, different meshes are used for each one. The central part of the inverse analysis relates the radiation transferred between the heater and the design surface, forming an ill-conditioned system of linear equations on the radiosities of the heater elements, which is ill-conditioned and has in general different numbers of equations and unknowns. The other terms of the energy equations are incorporated into the problem by an iterative procedure. The ill-conditioned nature of the system is treated by means of truncated singular value decomposition (TSVD), a regularization method that also permits the solution of problems having unequal number of unknowns and equations.

The proposed methodology is applied to a few example cases to demonstrate some typical characteristics of a radiation-convection combined mode inverse design.

2. Physical and Mathematical Model

Figure 1 presents a schematic view of a two-dimensional enclosure, which is formed by gray-diffuse surfaces. Due to symmetry, only one-half of the enclosure is shown. The space inside the enclosure is filled with air, a non-participating medium. Heat transfer is governed by thermal radiation exchange between the surfaces and by turbulent convective transfer between air and the surfaces. The design surface is located on the bottom, and the heaters are located on the top and/or side of the enclosure. The remainder of the enclosure is formed by walls that are assumed adiabatic. To reduce the computation effort, only one-half of the enclosure is simulated.

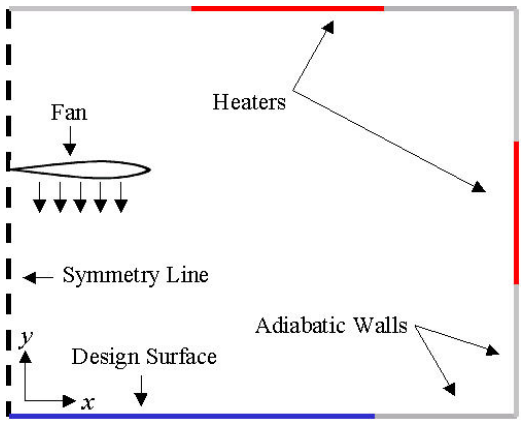

Figure 1. Schematic walls of the enclosure

To perform the numerical simulation, different discretizations of the domain are proposed, as depicted in Fig. 2. The thermal radiation grid mesh is shown in Fig. 2a, where the enclosure walls are divided into uniform-sized elements $\Delta x = \Delta y$, to which the energy balance is applied. Figure 2b shows the convection grid mesh, having non-uniform elements. The need to employ different meshes arises from the fact that turbulent convection requires considerable refinement close to the surfaces, which is not necessary for an accurate computation of thermal radiation and would demand an excessive computational time.

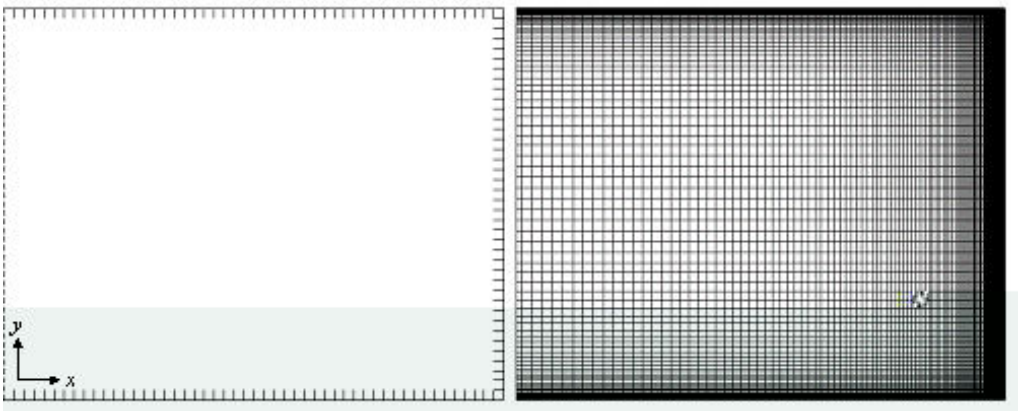

Figure 2. Discretization of the enclosure:
(a) thermal radiation mesh: finite areas; (b) turbulent convection mesh: control volumes.

The mathematical model of the radiation exchanges between the surfaces relies on the relations for enclosures (Siegel and Howell 2002). The problem is formulated by a system of integral equations, which can be solved numerically by the discretization of the domain into finite size elements. The element indices on the design surface, heater and adiabatic walls are designated by *jd*, *jh* and *jw*, while the number of elements on these surfaces are designated by JD, JH and JW, respectively. The radiative heat flux on a design surface element *jd* is given by a balance between radiosity and irradiation (both in W/m^2):

$$q_{r,jd} = q_{o,jd} - q_{i,jd} \tag{1}$$

The radiosity $q_{o,jd}$ accounts for both emission and reflection from the design surface element. Considering that the temperature and the radiative heat fluxes are specified on the design surface, the radiosity of the design surface element can be readily found from the relation:

$$q_{o,jd} = \sigma T_{jd}^4 - \frac{1-\varepsilon_d}{\varepsilon_d} q_{r,jd} \tag{2}$$

where T_{jd} is the absolute temperature of design surface element *jd*, in K, σ is the Stefan-Boltzmann constant, equal to 5.67×10^{-8} W/m^{2}K^4 and ε_d is the hemispherical emissivity of the design surface. The irradiation $q_{i,jd}$ accounts for all the incident radiative energy on the design surface element, including both emissions and reflections from the other surfaces of the enclosure, and is given by:

$$q_{i,jd} = \sum_{jh}^{\mathrm{JH}} F_{jd-jh} q_{o,jh} + \sum_{jw}^{\mathrm{JW}} F_{jd-jw} q_{o,jw} \tag{3}$$

In the above equation, F_{jd-jh} and F_{jd-jw} are respectively the view factors between elements on the design surface and on the heater and between elements on the design surface and on the wall; $q_{o,jh}$ and $q_{o,jw}$ are the radiosities of element *jh* on the heater and of element *jw* on the wall, respectively.

As stated before, no thermal condition has been imposed on the heater. At this point, however, it is possible to rearrange Eqs. (1) and (3) to provide an equation for the radiosity of the heater elements:

$$\sum_{jh=1}^{\mathrm{JH}} F_{jd-jh} q_{o,jh} = q_{o,jd} - q_{r,jd} - \sum_{jw=1}^{\mathrm{JW}} F_{jd-jw} q_{o,jw} \tag{4}$$

A radiative energy balance on the adiabatic wall elements leads to an equation for the radiosities $q_{o,jw}$:

$$q_{o,jw} = \sum_{jd=1}^{\mathrm{JD}} F_{jw-jd} q_{o,jd} + \sum_{jh=1}^{\mathrm{JH}} F_{jw-jh} q_{o,jh} + \sum_{jw^*=1}^{\mathrm{JW}} F_{jw-jw^*} q_{o,jw^*} \tag{5}$$

Finally the radiation formulation is completed by setting a relation for the net radiative heat flux on the heater elements:

$$q_{r,jh} = q_{o,jh} - \sum_{jd=1}^{\mathrm{JD}} F_{jh-jd} q_{o,jd} - \sum_{jw=1}^{\mathrm{JW}} F_{jh-jw} q_{o,jw} - \sum_{jh^*=1}^{\mathrm{JW}} F_{jh-jh^*} q_{o,jh^*} \tag{6}$$

In Eqs. (5), the last term on the right-hand side arises from the fact that an adiabatic wall element *jw* can "see" another adiabatic wall element *jw**, as shown in Fig. 1. The same applies to the last term of Eq. (6) regarding the heater elements *jh* and *jh**.

The computation of the heat transfer between the air and the surfaces requires the solution of the fluid flow and temperature field in the air. The fluid flow can be solved by time-averaged continuity and momentum equations in the *x* and *y* direction, as given by Bejan (1995) and Launder (1974):

$$\frac{\partial(\rho\overline{u})}{\partial x} + \frac{\partial(\rho\overline{v})}{\partial y} = 0 \tag{7}$$

$$\overline{u}\frac{\partial\overline{u}}{\partial x} + \overline{v}\frac{\partial\overline{u}}{\partial y} = \overline{X} - \frac{1}{\rho}\frac{\partial\overline{p}}{\partial x} + \frac{\mu}{\rho}\left(\frac{\partial^2\overline{u}}{\partial x^2} + \frac{\partial^2\overline{u}}{\partial y^2}\right) - \left(\frac{\partial\left(\overline{u'^2}\right)}{\partial x} + \frac{\partial\left(\overline{u'v'}\right)}{\partial y}\right) \tag{8}$$

$$\overline{u}\frac{\partial\overline{v}}{\partial x} + \overline{v}\frac{\partial\overline{v}}{\partial y} = \overline{Y} - \frac{1}{\rho}\frac{\partial\overline{p}}{\partial y} + \frac{\mu}{\rho}\left(\frac{\partial^2\overline{v}}{\partial x^2} + \frac{\partial^2\overline{v}}{\partial y^2}\right) - \left(\frac{\partial\left(\overline{u'v'}\right)}{\partial x} + \frac{\partial\left(\overline{v'^2}\right)}{\partial y}\right) \tag{9}$$

The momentum transport of the turbulent eddies is modeled by the Boussinesq hypothesis, given by:

$$-\overline{u'v'} = \frac{\mu_t}{\rho}\frac{\partial \overline{u}}{\partial y} \tag{10}$$

In the $\kappa - \varepsilon$ turbulence model, the momentum eddy-viscosity $\nu_t = \mu_t / \rho$ is computed from the relation $c_\mu \kappa^2 / \varepsilon$, where the values of κ and ε come directly from the differential transport equations for the turbulence kinetic energy and turbulence dissipation rate.

$$\overline{u}\frac{\partial \kappa}{\partial x} + \overline{v}\frac{\partial \kappa}{\partial y} = \left(\frac{\mu}{\rho} + \frac{\mu_t}{\rho \sigma_k}\right)\left(\frac{\partial^2 \kappa}{\partial x^2} + \frac{\partial^2 \kappa}{\partial y^2}\right) + \frac{\mu_t}{\rho}\left(\frac{\partial \overline{u}}{\partial y} + \frac{\partial \overline{v}}{\partial x}\right)\left(\frac{\partial \overline{u}}{\partial y}\right) - \varepsilon \tag{11}$$

$$\overline{u}\frac{\partial \varepsilon}{\partial x} + \overline{v}\frac{\partial \varepsilon}{\partial y} = \left(\frac{\mu}{\rho} + \frac{\mu_t}{\rho \sigma_\varepsilon}\right)\left(\frac{\partial^2 \varepsilon}{\partial x^2} + \frac{\partial^2 \varepsilon}{\partial y^2}\right) + c_{\varepsilon 1}\frac{\mu_t}{\rho}\frac{\varepsilon}{\kappa}\left(\frac{\partial \overline{u}}{\partial y} + \frac{\partial \overline{v}}{\partial x}\right)\left(\frac{\partial \overline{u}}{\partial y}\right) - c_{\varepsilon 2}\frac{\varepsilon^2}{\kappa} \tag{12}$$

where $c_\mu = 0.09$, $c_{\varepsilon 1} = 1.44$, $c_{\varepsilon 2} = 1.92$, $\sigma_\varepsilon = 1.3$ and $\sigma_k = 1$.

The energy equation can be written as:

$$\overline{u}\frac{\partial \overline{T}}{\partial x} + \overline{v}\frac{\partial \overline{T}}{\partial y} = \frac{\mu_t}{\mathrm{Pr}_t}\left(\frac{\partial^2 \overline{T}}{\partial x^2} + \frac{\partial^2 \overline{T}}{\partial y^2}\right) \tag{13}$$

where Pr_t is the turbulent Prandtl number, which relates the the momentum and the thermal eddy-viscosities, ν_t / α_t, and is taken as equal to 0.9 (Kays and Crawford, 1993).

Boundary conditions are required for all the conservation equations. On the walls, the non-slip and impermeability conditions are imposed, so $u = v = 0$, and the air temperature is set equal to the wall temperature. In the symmetry line, on the left, all gradients in the x-direction are null, $\partial(\,)/\partial x = 0$. On the control volumes occupying the position where the fan blades are located, a downward velocity v is prescribed.

3. Solution Procedure

3.1. Regularization of the System of Equations

In inverse analysis of purely radiative heat transfer processes, the prescribed heat flux on the design surface is equal to the radiative heat flux. This is the starting point of the inverse solution, for the radiosity in the design surface can be directly computed from Eq. (2) with the known temperature and radiative heat flux. In combined heat transfer mode, the prescribed heat flux is a combination of the radiation and convection mechanisms:

$$q_{t,jd} = q_{r,jd} + q_{c,jd} \tag{14}$$

Therefore, the radiative heat flux on the design surface is no longer the same as the prescribed heat flux; in fact both the radiative and the convective heat flux are unknown, and need to be found from the solution of the governing equations.

To allow the use of the pure radiative inverse design methodology, it is proposed here to use an iterative procedure in which the convective flux is initially guessed followed by a radiative heat flux computed from Eq. (14). Next, the radiosities of the design surface elements are determined from the application of Eq. (2). The energy balance for the design surface is taken to form a system of linear equations to solve for the unknown radiosities of the heater elements, as given by Eq. (4). This system has two challenging aspects. First, the number of equations is equal to the number of design surface elements, JD, while the number of unknowns is equal to the number of heater elements, JH. Therefore, unless JD and JH are equal, the numbers of equations and of unknowns are not the same. Secondly, the system is expected to be ill-conditioned due to its inverse nature. The application of conventional methods of matrix inversion inevitably leads to a solution vector whose components present steep oscillations between positive and negative numbers, which is not physically acceptable since the radiosities must be positive numbers.

The above two difficulties can be dealt with through the application of so-called regularization methods. Such methods impose additional constraints to the original problem to smooth the solution vector, although at the expense of introducing an error into the solution. Well known methods include techniques based on singular value decomposition (SVD), schemes using Tikhonov regularization, and conjugate gradient regularization methods.

In this work, the truncated singular value decomposition (TSVD) was the selected method. First, matrix **A**, corresponding to the set of Eqs. (4), and whose components are the view factors F_{jd-jh}, is singularly decomposed into three matrices:

$$\mathbf{A} = \mathbf{U}\mathbf{W}\mathbf{V}^T \tag{15}$$

where **U** and **V** are orthogonal matrices, and **W** is a diagonal matrix formed by the singular values w_j. The solution vector **x**, which is formed by the radiosities of the heater elements, is computed by:

$$\mathbf{x} = \sum_{j=1}^{\mathrm{JH}} \left(\frac{b_k \cdot u_{kj}}{w_j} \right) \mathbf{v}_j \tag{16}$$

In ill-posed problems, the singular values w_j decay continuously to very small values. Since they are in the dominator of Eq. (16), this results in components of **x** with very large absolute numbers. However, the smaller the singular value w_j is, the closer the corresponding vector v_j is to the null-space of **A**. In other words, the terms related to the smaller singular values can be eliminated from Eq. (16), without introducing a large error to the solution. This is the main idea of the TSVD: only the terms related to the *p*-th largest singular values are kept on Eq. (16), instead of all JH terms. The solution is the vector **x** with the smallest norm subjected to minimum deviation $|\mathbf{A} \cdot \mathbf{x} - \mathbf{b}|$. Another important feature of the TSVD method is that it can also be applied to the case where the numbers of unknowns and equations are not the same, as will be discussed in the Results section.

3.2. Solution Strategy

The first step consists of dividing the computational domain into control volumes for the solution of the convection process, and dividing the surfaces into equal-size areas for the solution of the radiation exchange relations. On the design surface, both the temperature and the total heat flux are prescribed. The solution is based on the following steps:

1. The convective heat fluxes on the design surface elements, $q_{c,jd}$, are guessed (starting with $q_{c,jd}$ = 0), and the radiative heat fluxes on design surface elements $q_{r,jd}$ are computed from Eq. (14).
2. The radiosities of the adiabatic wall elements, $q_{o,jw}$, are guessed (starting with $q_{o,jw}$ = 0).
3. The radiosities of the design surface elements, $q_{o,jd}$, are computed from Eq. (2). Equation (4) is written for all JD design surface elements to solve for the JH radiosities of the heater elements, $q_{o,jh}$. The system of equations is solved for $q_{o,jh}$, and the radiosities $q_{o,jw}$ are recalculated from the application of Eq. (5) to the JW wall elements (forming a well-conditioned system of linear equations with JH unknowns and equations).
4. Step 3 is repeated, redoing the calculations with the new values of $q_{o,jw}$ until the radiosities $q_{o,jh}$ converge with a maximum relative deviation of 10^{-6} between the last two iterations.
5. Equation (6) is applied to the JH heater elements to find the net radiative heat fluxes, $q_{r,jw}$, on the heater elements. The application of the radiative relations also allows the determination of the temperature distribution on the heater and on the adiabatic walls. At this point, the inverse solution is complete for the imposed values of $q_{r,jd}$, which was computed from the guessed values of $q_{c,jd}$ (in Step 1).
6. With the obtained temperature distribution on the enclosure surfaces, the convective governing equations given by Eqs. (7) through (13) provide a means for determining the convective heat fluxes on all surfaces of the enclosure.
7. Step 1 is repeated, redoing the calculations with the new values of $q_{c,jd}$ until $q_{r,jd}$ converges with a maximum relative deviation of 10^{-6} between the last two iterations.

Combined radiation-convection heat transfer problems are known to be generally difficulty to converge. To allow convergence of the proposed method, the convective heat fluxes $q_{c,jd}$ were under-relaxed in Step 7 with a factor of 0.05. The adiabatic walls elements radiosities, $q_{o,jw}$, are under-relaxed in Step 3 with a factor of 0.1.

3.3. Verification of the Solution

The application of TSVD regularization inevitably introduces an error to the solution, since only $p < \mathrm{JH}$ terms are kept in the series of Eq. (16). Verification of the inverse solution is straightforward. With the obtained total heat fluxes

on the heaters, a forward problem in which the temperatures on the design surface elements and the total heat fluxes on the heaters and adiabatic walls are known is run to find the total heat flux on the design surface, $q_{t,jd}$, which can be compared with the prescribed heat flux, $q_{\text{prescribed}}$, by:

$$\gamma_{\max} = \max_{jd} \left| \frac{q_{t,jd} - q_{\text{prescribed}}}{q_{\text{prescribed}}} \right| \tag{17}$$

4. Results and Discussion

The system considered in this work is the two-dimensional enclosure shown in the schematic of Fig. 1. The total hemispherical emissivities of the design surface, of the heater and of the walls are $\varepsilon_d = \varepsilon_h = \varepsilon_w = 0.8$. Taking advantage of the symmetry, only one-half of the domain is solved. The dimensions of the enclosure in Fig. 1 are L = 0.70 m and H = 0.56 m. It is specified that the temperature and total heat flux on the design surface be respectively $T_{prescribed} = 673\,\text{K}$ and $q_{prescribed} = -3.220 \times 10^3\ \text{W/m}^2$. The negative sign follows from the heat transfer convention that heat going out of a system is positive. The results are presented in dimensionless form: the dimensionless temperature and heat flux are defined by $t = T / T_{ref}$ and $Q = q / \sigma T_{ref}^4$, where the reference temperature is $T_{ref} = 1173\,\text{K}$. Therefore, for the design surface, the prescribed conditions are $t_{prescribed} = 0.574$ and $q_{prescribed} = -0.3$. A few solutions for the heat flux distribution on the heaters are presented next.

Figure 3 presents Case 1. It is considered that the heater occupies the entire extension of the top surface, while the right-side surface is adiabatic. The design surface is located on the bottom of the enclosure, but is kept at some distance from the right corner; in previous studies (França et al., 2003) it was shown that the portion of the design surface close to the corner is much less affected by the heater than by the adiabatic surface itself. Placing design surfaces on the right side, near the adiabatic wall would makes it much more difficult, if not impossible, to find a satisfactory solution on the heater. As shown in Fig. 2a, the radiation mesh was divided into 50 and 40 uniform-sized elements in the x and y directions, so that the dimensionless sizes of the surface elements were $\Delta x/L = \Delta y/L = 0.02$. For the convection part, shown in Fig. 2b, the mesh was divided into 120 and 90 elements in the x and y directions, respectively. To capture the steeper variation of temperature and fluid velocities close to the surfaces, as observed in turbulent flows, a non-uniform mesh was adopted using the same hyperbolic functions presented in Davidson (1990). For all cases presented in this paper, the solutions proved to be grid independent for these two mesh configurations.

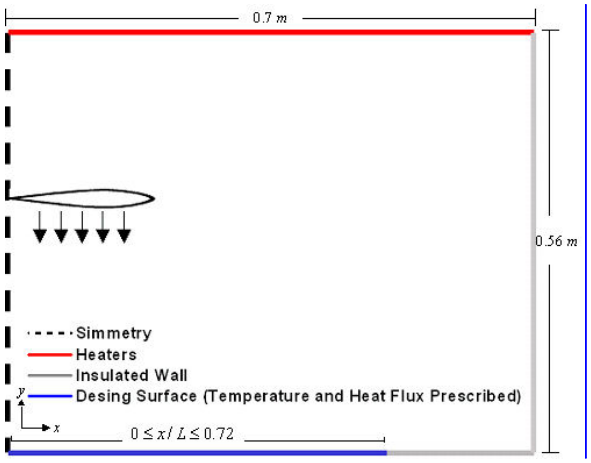

Figure 3: Design surface and heater configurations for Case 1.

For a better understanding of the effect of the convective heat transfer, a purely radiative enclosure is first solved, in which no flow is provided by the fan and free convection is neglected. In this case, the total radiative heat flux is equal to the total heat flux. The problem is modeled by a system of linear equations, as described in Sections 2 and 3. For the pure radiation problem the numbers of computational area elements on the design surface and on the heater are JD = 36 and JH = 50, respectively. For this choice of design surface and heater elements the number of equations, equal to JD, and the number of unknowns, equal to JH, are not the same as is typical in inverse design problems. The application of the TSVD regularization to the system of equations results in the singular values shown in Fig. 4 with the label Case 1. A total of JH = 50 singular values are generated, but only the first 36 values (the same as the number of equations, JD) are non-zero, which are the ones shown in Fig. 4. The steep decay of the singular values indicates the ill-conditioned characteristics of the system of equations. Keeping all the terms of the series of Eq. (16) results in negative values for

the radiosities $q_{o,jh}$, a non-physically acceptable solution. The TSVD regularization eliminates the high-order terms of the series to smooth the solution and recovers positive values for the radiosities $q_{o,jh}$. Figure 5 presents the total heat flux on the heater elements when keeping only two (p = 2) and three (p = 3) terms of the series. Setting a larger number of terms resulted in negative heat fluxes (a non practical solution) or negative radiosities (a physically unacceptable solution) on the heaters. The resulting heat fluxes on the design surface, computed from the procedure described in Section 3.3, are also shown in the figure for the solutions with p = 2 and p = 3. As seen, despite eliminating most of the terms of the series of Eq. (16), it was possible to obtain very different solutions for the heater that were capable of satisfying the desired heat flux on the design surface with a small error, as given by Eq. (17): for p = 2, γ_{max} = 0.84 %; for p = 3, γ_{max} = 0.10 %. Figure 5 also shows the heat flux on the adiabatic surface on the bottom surface, which was set equal to zero.

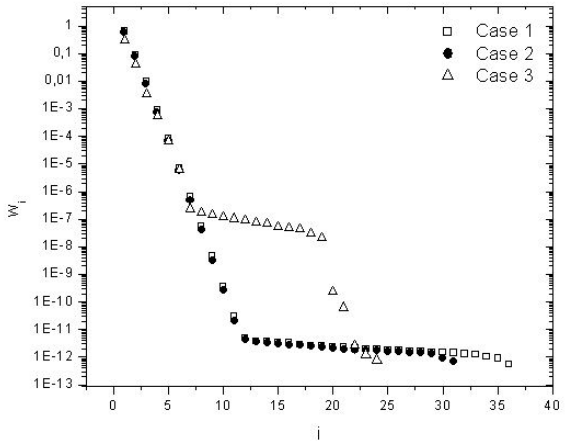

Figure 4: Singular values for different solution cases

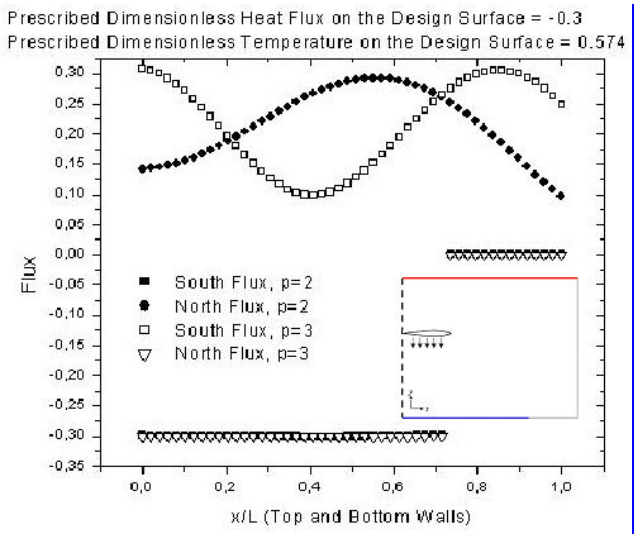

Figure 5: Solution for purely radiative heat transfer
(marked with the red line on the top surface of the schematic presented in the figure)

In the above case, the total heat fluxes on the heater and on the design surfaces are solely radiative, since convection was neglected. The more complex case of a coupled radiation convection problem is now discussed. It is assumed that the fan is operated to generate a typical air flow velocity of 4 m/s, normal to the cross-sectional area of the fan. The proposed combined mode inverse solution procedure described in Section 3 was applied. Keeping the same heater and design surface configurations of Fig. 3, the singular values are the same of the purely radiative problem, labeled as Case 1. In the presence of flow, all attempts of recovering a heat flux on the heater for this configuration failed. Even after reducing the number of terms in the Series of Eq. (16), it was not possible to avoid negative values for the radiosities on the heater elements. A close analysis of the problem revealed that a stagnation region exists in the region close to the symmetry line; the convective heat transfer is relatively higher than in the other regions of the design surface. Since the total heat flux is prescribed to be uniform, it follows from Eq. (14) that the radiative heat flux on the

design surface in the region close to the symmetry line must be considerably smaller than in the other regions of the design surface. This restriction made the inverse solution for the heater heat fluxes unviable. This illustrates another characteristic of inverse problems: Just specifying conditions on the design surface does not guarantee that a useful solution exists.

As an attempt to avoid the above difficulty, a new proposition for the design surface was considered, as shown in Fig. 6. In this case, only the temperature condition was prescribed on the portion of design surface close to the symmetry line, while the heat flux was left unconstrained, and will be determined from the specification of the heater that will lead to uniformity of temperature on the design surface. Since the size of the design surface was reduced, keeping the same grid resolution, the number of elements on the design surface was reduced to JD = 31, the same as the number of equations of the system of equations. The singular values of the system are shown in Fig. 4 under label Case 2. Only the 31 non-zero singular values (from the total of 50) are shown in the figure. In this case, it was only possible to recover a physically acceptable solution (that is, positive radiosities on the heater elements) keeping two terms in the series of Eq. (16), $p = 2$. The solution for the total heat distribution on the heater is shown in Fig. 7. The figure also presents the radiative and the convective heat flux. As seen, for these conditions, the heat flux on the heater is dominated by thermal radiation, although the convection heat transfer is an important mechanism to be considered. While the solution is physically acceptable, in the sense that the radiosities of the heater elements are positive, it is not practical, since the total heat flux is negative close to the symmetry line, a result that is not acceptable for a heater design.

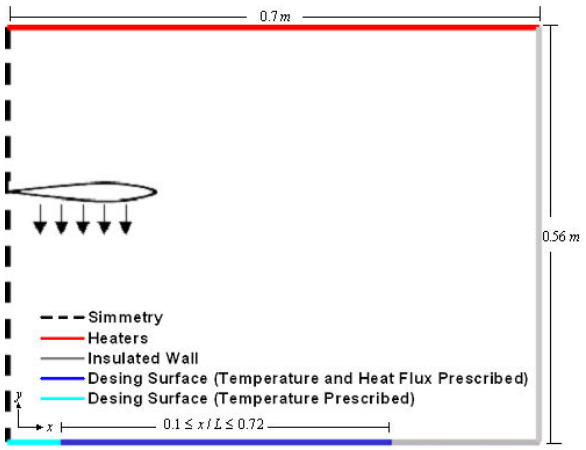

Figure 6: Design surface and heater configurations for Case 2.

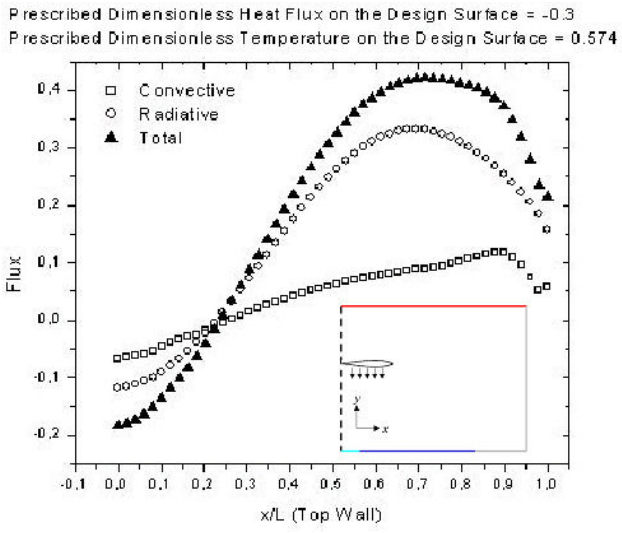

Figure 7: Heat flux on the heater surface. Case 2.
(marked with the red line on the top surface of the schematic presented in the figure)

To eliminate negative heat fluxes on the heater elements, other configurations of the heaters were attempted. One of them is shown in Fig. 8, where the heaters are located on the top and both side surfaces. The heater is placed in the center of the top and side surfaces as well as close to the top corner. All the other conditions were maintained the same

as in the previous case. The number of elements in the design surface is again JD = 31, while the number of heating elements is now JH = 27. Thus the system of equations is over constrained with JD = 31 equations and JH = 27 unknowns. The singular values are shown in Fig. 4 under label case 3. For this case, it was possible to recover a physically acceptable solution keeping only the first two terms in the series of Eq. (16). Figures 9 and 10 show the total heat flux, as well as its radiative and convective components, for the heaters on the top and left surfaces, respectively. As seen, in all heater elements the total heat flux is positive, which characterizes a satisfactory solution. The heat transfer is dominated by thermal radiation, although the contribution of the convective mechanism is still important. Figures 9 and 10 also show the radiative and convective heat fluxes on the adiabatic surfaces of the top and left surfaces. Note that the adiabatic condition imposes that the total heat transfer be null, so that the sum of the radiative and convective heat fluxes is zero, as shown in Figs. 9 and 10.

Figure 11 presents the heat transfer on the bottom surface, where the design surface is located. In the region defined by $0.1 < x/L < 0.7$, where the condition of total dimensionless heat flux of $q_{t,jd} = -0.3$ was imposed, the maximum error of the inverse solution, given by Eq. (17), was $\gamma_{max} = 7.26\%$. In the region defined by $x/L < 0.1$, where only the temperature condition of $t_{jd} = 0.574$ was imposed, the total heat flux presents a deviation from the required heat flux, reaching a maximum error of $\gamma_{max} = 10.19\ \%$. Figure 11 also shows the heat fluxes on the adiabatic surface located in the proximity of the right corner on the bottom. As required, the total heat flux, given by the sum of the radiative and the convective heat fluxes, is zero.

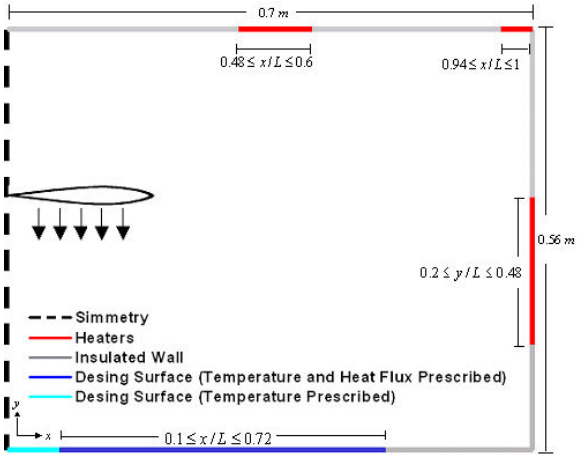

Figure 8: Design surface and heater configurations for Case 3.

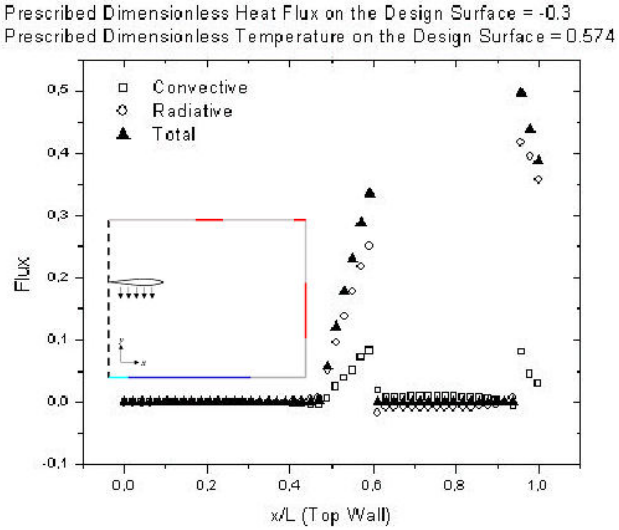

Figure 9: Heat flux on the top surface. Case 3.
(marked with the red line on the top surface of the schematic presented in the figure)

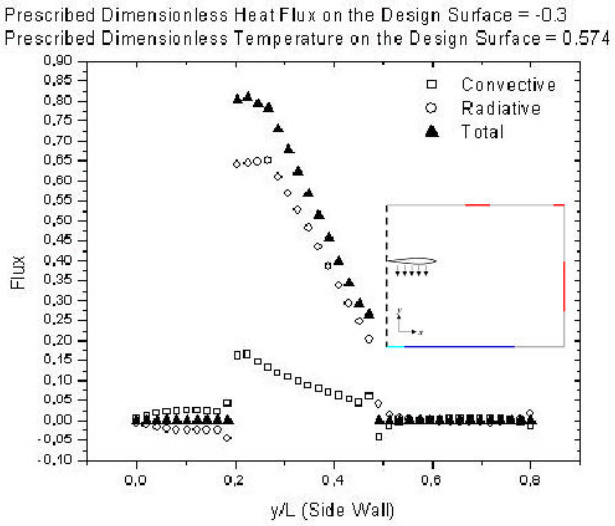

Figure 10: Heat flux on the side surface. Case 3.
(marked with the red line on the side surface of the schematic presented in the figure)

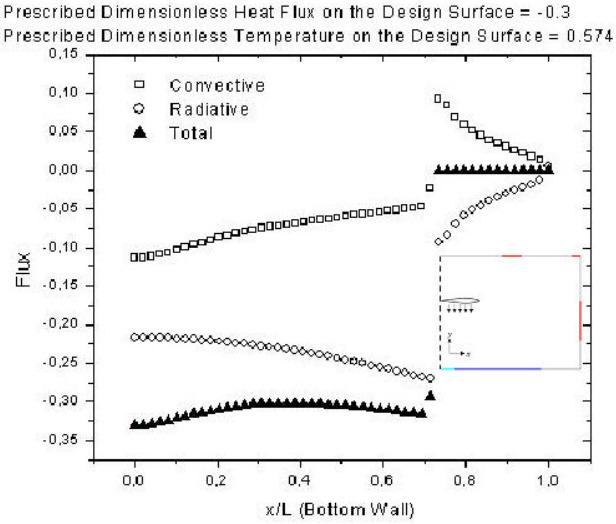

Figure 11: Heat flux on the bottom surface Case 3.
(marked with the blue line on the bottom surface of the schematic presented in the figure)

Comparing the heat fluxes on the design surface in Figs. 5 and 11 indicates that, for the proposed oven configuration, attaining uniformity of heat flux and temperature on the design surface was much more difficult for the case of combined convection-thermal radiation than for the pure radiative heat transfer case. For the proposed enclosure configuration, the fan axis is in the symmetry line and blows air directly to the design surface. Figures 12 and 13 show the air velocity and temperature fields, respectively, for Case 3. As seen in Fig. 12, air circulates in a counterclockwise rotation, forming a stagnation region near the symmetry line and causing the largest temperature gradients on the design surface. It follows that the convective heat flux, given by Fourier's conduction law in the limit where $y \rightarrow 0$, is also the largest in this region. The detailed view in Fig. 13 shows the isotherms close to the interface between the symmetry line and the design surface. It can be observed that the temperature gradient (and the convective heat flux, as seen in Fig. 11) decreases as one moves away from the symmetry line. For this reason, the convective heat flux is larger in the region close to the symmetry line, and the radiative heat flux is smaller. This non-uniformity of the radiative heat flux proved to be a decisive difficulty for the solution of this problem. To obtain results with smaller errors than are found in this case, it may be necessary to change the location of the fan or impose a different direction for the rotation of the air flow, avoiding the stagnation region in the symmetry line.

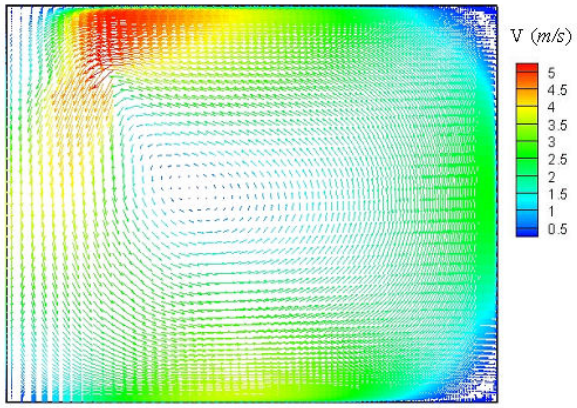

Figure 12: Velocity field in the air flow for Case 3.

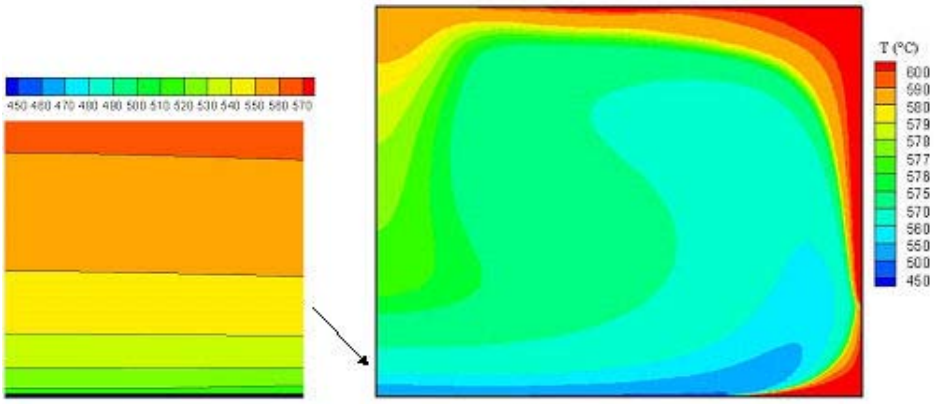

Figure 13: Temperature field in the air flow for Case 3.

5. Conclusions

This paper presented the application of the inverse design technique to determine the power input in the heaters of a two-dimensional convective-radiative oven to attain uniformity of temperature and heat flux on the design surface. The central part of the inverse analysis was assembled to relate the heaters directly to the design surface. This led to an ill-conditioned system of linear equations on the heater elements radiosities. Reflections of radiative energy from the adiabatic walls and the heat transferred from the turbulent air flow were incorporated into the formulation by an iterative procedure. As expected, the resulting system of equations was ill-conditioned. The regularization method chosen was truncated singular value decomposition (TSVD), a method that also permitted the solution of a problem that was characterized by unequal numbers of unknowns and equations.

The proposed methodology was applied to a few example cases to demonstrate some typical characteristics of a combined mode inverse design. The first case consisted of a purely radiative enclosure. In this case, two regularized solutions were obtained that satisfied the prescribed heat flux with an error less than 1.0 %. The cases considering combined radiation-convection heat transfer proved to be more difficult. For the proposed oven configuration, having the fan located in the symmetry line and blowing air directly to the center of the design surface caused the inverse solution to fail, due to the resulting low radiative heat flux required on the center relative to the other positions on the design surface. To obtain an acceptably practical solution, the heat flux on the design surface close to the symmetry line was left unconstrained. For this case, it was possible to obtain an acceptable power input in the heaters, although the maximum error increased to 10 %. For future work, it may be necessary to change the position of the fan and/or the direction of the air flow to avoid the stagnation region on the design surface. The heater positions were determined from observing the points of maximum required heat flux. So another important advance in the research would be establishing a methodology to solve automatically for the heater positions

Even with the difficulty in extracting physically meaningful results for some of the proposed cases, there was clear benefit in formulating this design problem in an inverse sense. There was added insight into the reasons why some problems failed which may not have been evident from a purely forward posed design formulation. The insights that are available in posing design problems in an inverse sense cannot be over-emphasized, in particular for difficult problems where the problem statement and associated physics are inherently uninvertible (i.e., having no physical forward equivalent).

6. Acknowledgments

The authors thank CAPES (Brazil) for the support under the program CAPES/UT-AUSTIN, No. 06/02, and to the contributions of profs. John R. Howell and Ofodike A. Ezekoye, from the University of Texas at Austin, by means of discussion and exchange of ideas during the execution of the work.

7. References

Bejan, A., and Jones, J. A.,1995, "Convection heat transfer", 2nd Ed, John Wiley and Sons, New York.

Launder, B. E., and Spalding, D. B., 1974, "The numerical computation of turbulent flow", Computational Methods for Applied Mechanical Engineering, vol. 3, p. 269.

Huang, C. J., Yu, C. C., and Shen, S. H., 2000, "Selection of measurement locations for the control of rapid thermal processor", Automatica, vol 36, pp. 705-715.

França, F., and Howell, J., 2006, "Transient Inverse Design of Radiative Enclosures for Thermal Processing of Materials," Inverse Problems in Science and Engineering, pp. 1-14.

França, F., Howell, J., Ezekoye, O., and Morales, J. C., 2003, "Inverse design of thermal systems", *Advances in Heat Transfer*, Vol. 36, pp. 1-110.

Daun, K., França, F., Larsen, M., Leduc, G., and Howell, J. R., 2006, "Comparison Methods for Inverse Design of radiant Enclosures," Journal of Heat Transfer, Vol. 259, pp. 269-282.

Davidson, L., 1990, "Second order corrections of the $k-\varepsilon$ model to account for non-isotropic effects due to buoyancy", International Journal of Heat and Mass Transfer, vol. 33, pp. 2599-2608.

Hansen, P. C., 1990, "Truncated SVD solutions to discrete ill-posed problems with ill-determined numerical rank", SIAM J. Sci. Statist. Comput., Vol 11, pp. 503-518.

Siegel, R., and Howell, P. C., 2002, "Thermal radiation heat transfer", 4th Ed., Taylor and Francis, New York.

Kays, W. M., and Crawford, M. E., 1993, "Convective heat and mass transfer", McGraw-Hill, New York.

8. Copyright Notice